

Network Security under Heterogeneous Cyber-Risk Profiles and Contagion

Elisa Botteghi¹, Martino Centonze¹, Davide Pastorello^{1,2}, and Daniele Tantari¹

¹ Department of Mathematics, University of Bologna

² TIFPA-INFN, via Sommarive 14, 38123 Povo TN (Italy)

daniele.tantari@unibo.it

Abstract. Cyber risk has become a critical financial threat in today’s interconnected digital economy. This paper introduces a cyber-risk management framework for networked digital systems that combines the strategic behavior of players with contagion dynamics within a security game. We address the problem of optimally allocating cybersecurity resources across a network, focusing on the heterogeneous valuations of nodes by attackers and defenders, some areas may be of high interest to the attacker, while others are prioritized by the defender. We explore how this asymmetry drives attack and defense strategies and shapes the system’s overall resilience. We extend a method to determine optimal resource allocation based on simple network metrics weighted by the defender’s and attacker’s risk profiles. We further propose risk measures based on contagion paths and analyze how propagation dynamics influence optimal defense strategies. Numerical experiments explore risk versus cost efficient frontiers varying network topologies and risk profiles, revealing patterns of resource allocation and cyber deception effects. These findings provide actionable insights for designing resilient digital infrastructures and mitigating systemic cyber risk.

Keywords: Network security · Security investments · Game theory · Contagion · Cyber risk propagation.

1 Introduction

Cyber risk refers to the potential for damage to digital systems and infrastructure, whether in terms of functionality or data integrity, resulting from security breaches.

In today’s digital economy, cyber risk is inherently a financial risk. Firstly, cyber-attacks translates into financial losses because operational disruptions and data breaches directly impact assets of economic value [15]: operability itself has financial worth, and data are increasingly treated as valuable commodities. Secondly, modern financial systems are tightly interwoven with digital infrastructures—commonly referred to as cyber-physical systems—where a cyber infection at the digital layer can escalate into the financial domain, potentially propagating across institutions and triggering systemic instability [14,26]. For

example, [30,31] document cases in which cyberattacks targeting technology service providers, such as digital payment platforms, led to liquidity crises within interbank networks. Additional spillover effects include adverse stock market reactions and reputational damage following cyber incidents. [12,22,45,4,25,3]. As a result, effective cyber-risk management and strategic investment in cybersecurity are essential not only for digital resilience but also for the broader stability of financial systems.

As digital ecosystems become increasingly complex, the need to manage large amounts of data has led to infrastructures that are typically organized as networks of interconnected servers or units. While such interconnectivity enhances efficiency, scalability, and redundancy, it also introduces systemic vulnerabilities: a single breach can act as a gateway for contagion, allowing malicious activity to propagate and potentially compromise the entire system.

In this work, we propose a cyber risk management framework for digital networked systems, designed to identify an optimal investment strategy for allocating cybersecurity defenses across network nodes. The core components of our model include contagion across the network and the strategic behavior of cyber attacks.

For the first component, we draw inspiration from the extensive literature on complex networks [42,51,34]. Complex network models of contagion have been widely applied to biological [44,13], social [41,21], and financial systems [19,2,9,10], where the propagation of shocks or behaviors is mediated by the structure of interactions among agents. Typically, these models assume that the initial trigger—be it the zero-patient of an epidemic, a financial shock, or a rumor—is exogenous and random, reflecting events that are unintentional and difficult to predict or control.

However, this assumption does not hold in the context of cybersecurity, where attacks are often strategic and targeted. To address this, we adopt a game-theoretic framework, building on the literature of security games [52,47,36,39], which explicitly models the adversarial nature of cyber threats and the strategic allocation of defenses.

In particular, two players Stackelberg security games [49]-in which a defender (leader) commits to a defensive strategy and an attacker (follower) responds accordingly- have received significant interest due to their wide range of applications including patrolling tasks [48,8,46], environmental protection efforts [17,16] and defense coordination [20,27]. Within this framework, security games that incorporate interdependencies among nodes—where insufficient protection of one node can undermine the defense of its neighbors—have been studied in [38,11,35]. Multi-step attacks propagating through the system have been extensively studied using the formalism of attack graphs [28,57].

Models that explicitly account for contagion phenomena, where threats propagate across the network, have been also examined in [5,33,1,53,7,6,23]. Most of these models, still grounded in an epidemiological view of contagion, assume that the attacker’s objective is simply to maximize the spread of infection across the network. However, in cybersecurity settings, the attacker may instead aim to

reach specific nodes or regions considered strategic or of higher value. Similarly, the defender may prioritize the protection of critical nodes while allowing others to be sacrificed.

In our work, building on the contagion mechanism of [5,1], we therefore consider a heterogeneous network in which both attacker and defender assign values to each node and a corresponding target risk. The attacker and defender may assign different value/risk profiles to the nodes, reflecting their asymmetric information and differing perspectives on the system’s structure and strategic importance. The two players compete within a security game with limited budget: the defender strategically allocates cybersecurity resources across the network nodes, while the attacker determines an optimal probability distribution over potential targets.

The main contributions of this paper are organized as follows. In Section 2, we introduce the general setting. Section 2.1 defines the static contagion mechanism adopted. In Section 2.2, we present the security game framework, including the attacker’s and defender’s value/risk profiles. Section 2.3 recalls the Stackelberg formulation of the game and the corresponding definition of Strong Stackelberg Equilibria.

Section 3 outlines the main analytical results. In Section 3.1, we provide a characterization of the Stackelberg equilibrium based on intuitive and naturally emerging network metrics. These metrics quantify the extent to which each node contributes to the overall protection of the system and are combined in a principled way according to the players’ respective risk profiles. Section 3.2 introduces a class of risk measures defined in terms of the number of contagion paths, allowing for the inclusion of a dynamic parameter linked to propagation time.

Section 4 discusses the numerical results. In Section 4.1, we use the efficient frontier to compare the overall system robustness to strategic attacks across different network topologies and risk profiles. Section 4.2 analyzes examples of optimal resource allocation patterns, with a focus on the emergence of cyber deception effects. In Section 4.3, we examine the robustness of the optimal strategies to model misspecifications across a range of different dynamic contagion mechanisms.

Finally, Section 4.3 presents the conclusions and outlines future research directions. The proof of the main theorem is provided in Appendix 5.

2 Model

2.1 Contagion on Networks

Let us consider an undirected network \mathcal{G} of n interconnected nodes represented by its adjacency matrix $\mathbf{A} = (A_{ij})_{i < j}^n$, $A_{ij} \in \{0, 1\}$, $i, j = 1, \dots, n$. Each entry A_{ij} encodes the presence ($A_{ij} = 1$) or absence ($A_{ij} = 0$) of a link between the pair of nodes (i, j) .

Each node s can be the target of a cyber-threat with a probability $\phi_s \in [0, 1]$, becoming the *seed* of a potential infection. Therefore, the cyber-attack distribution is represented by the vector $\phi = (\phi_i)_{i=1}^n, \sum_{i=1}^n \phi_i = 1$.

Nodes can be either immune or susceptible to cyber-attacks. We introduce the susceptibility vector $\mathbf{X} = (X_i)_{i=1}^n$, where each $X_i \in \{0, 1\}$ indicates whether node i is susceptible ($X_i = 1$) or immune ($X_i = 0$) to a cyber-threat. We model \mathbf{X} as a random vector of independent Bernoulli variables, with $\mathbb{P}(X_i = 0) = q_i$ and $\mathbb{P}(X_i = 1) = 1 - q_i$, where $q_i \in [0, 1]$. The vector $\mathbf{q} = (q_i)_{i=1}^n$ represents the *security level* of the system, with q_i denoting the security level of node i . The vector \mathbf{q} reflects how cybersecurity investments have been distributed across the network.

All model stochasticity is encoded in the probability space defined by the set of elementary events $(s, \mathbf{X}) \in \mathbb{N}_n \times \{0, 1\}^n =: \Omega$ together with the joint probability distribution

$$p(s, \mathbf{X}) := \phi_s \prod_{i=1}^n (1 - q_i)^{X_i} q_i^{1-X_i}, \quad (1)$$

where we assume that the seed location and the susceptibilities are independent random variables.

A security breach at a node poses a threat to its neighbors, potentially allowing a cyber-infection to spread throughout the entire system, starting from the initial seed. Since the infection propagates only through susceptible nodes, any susceptible node that is connected to the seed via a path consisting entirely of susceptible nodes will become infected. Alternatively, we can define the *transmission network* $\mathcal{T}(\mathbf{X})$ as the (random) sub-network of \mathcal{G} consisting only of susceptible nodes. Then, a node i becomes infected if and only if it belongs to the same connected component as the seed s in the transmission network, i.e. if there exists a path $i \sim s$ between i and s entirely in $\mathcal{T}(\mathbf{X})$. The infection condition can be simply expressed by the following

Definition 1 (Infected nodes). *Given a realization of the random vector \mathbf{X} and a seed s , a node i is said to become infected if there exists $\ell \in \mathbb{N}$ such that*

$$(\mathbf{A} \circ \mathbf{X} \mathbf{X}^T)_{is}^\ell \geq 1,$$

where \circ denotes the element-wise (Hadamard) product, i.e., $(\mathbf{A} \circ \mathbf{X} \mathbf{X}^T)_{ij} = A_{ij} X_i X_j$.

Let us stress that $\mathbf{A} \circ \mathbf{X} \mathbf{X}^T$ is the adjacency matrix of $\mathcal{T}(\mathbf{X})$ so $(\mathbf{A} \circ \mathbf{X} \mathbf{X}^T)_{is}^\ell$ is the number of paths of length ℓ from s to i in $\mathcal{T}(\mathbf{X})$. Note that the previous definition is entirely static, as it does not involve any specification of contagion dynamics or propagation time. Nonetheless, it can be interpreted as the asymptotic infection condition of any contagion dynamics—deterministic or stochastic—that propagates through the network links and that does not allow infected nodes to recover.

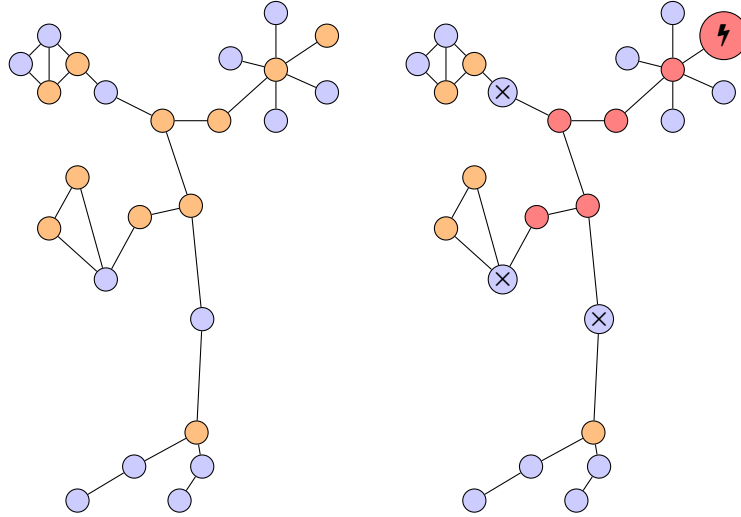


Fig. 1. Representation of the contagion process. Left panel: a realization of the network showing susceptible nodes (orange) and immune nodes (blue) before the attack; Right panel: after the attack all the susceptible nodes connected to the seed become infected (red). Strategically placed immune nodes can block the spread and protect other susceptible nodes from infection.

2.2 Security Game Framework

On top of this environment we consider a two players extensive game involving an attacker and a defender. The attacker optimizes the cyber-attack distribution vector ϕ , strategically selecting the nodes where it is most advantageous to pose a threat. The defender allocates cyber defenses across the network by adjusting the system's security vector q , aiming to identify an optimal cybersecurity investment strategy. Therefore, we refer to q and ϕ as defender and attacker *strategies* respectively.

The attacker's utility function \mathcal{U}_a and the defender's loss function \mathcal{L}_d , which are to be optimized, are defined with the following risk/cost structure:

$$\mathcal{U}_a(\phi; q) = \sum_i^n \eta_i \mathcal{R}_i(q, \phi; \mathbf{A}) - \theta \mathcal{C}_a(\phi), \quad (2)$$

$$\mathcal{L}_d(q; \phi) = \sum_i^n z_i \mathcal{R}_i(q, \phi; \mathbf{A}) + \alpha \mathcal{C}_d(q). \quad (3)$$

The strategy costs incurred by the attacker and the defender are denoted by $\mathcal{C}_a(\phi)$ and $\mathcal{C}_d(q)$, respectively. While $\mathcal{C}_d(q)$ concretely measures the size of investments in cyber defenses, $\mathcal{C}_a(\phi)$ has to be interpreted more as an information cost that penalizes low entropy attacking strategies concentrated on a limited subset of nodes. In the following, we assume either quadratic cost functions of

the form $\mathcal{C}_d(\mathbf{q}) = \frac{1}{2} \sum_{i=1}^n q_i^2$ and $\mathcal{C}_a(\phi) = \frac{1}{2} \sum_{i=1}^n \phi_i^2$, for analytical tractability, or alternatively L^1 -type penalizations to promote strategy sparsity. The hyper-parameters α and θ control the relative weight assigned to the cost terms and can be interpreted as Lagrange multipliers in a constrained optimization framework, where the attacker and the defender operate under limited budget constraints.

The vector $\mathcal{R} = (\mathcal{R}_i)_{i=1}^n$ in (2–3) measures the infection risk at each node, as a function of both the network structure \mathbf{A} and the strategies adopted by the two players (\mathbf{q}, ϕ) , thereby defining the system's *risk profile*. In the following, we analyze two distinct risk measures: the first is based on the actual probability of a node being infected, while the second relies on the expected number of paths connecting the node to the infection seed. The former enhances the interpretability of the optimal solution, whereas the latter improves its scalability.

Most models addressing contagion dynamics on complex networks are inspired by epidemiological frameworks. They often tacitly assume that the attacker's objective, either explicitly or as a natural consequence of viral replication, is to maximize damage to the network, merely intended as the overall size of the infection. In a cybersecurity context, a networked system is a heterogeneous collection of assets with varying levels of value. Consequently, each node contributes differently to the overall damage assessment. Moreover, the attacker and the defender may assign different values to the same node, either due to conflicting preferences or because of an information asymmetry between the node's actual value and the attacker's perceived value. For this reason, we introduced in (2–3) the *value profiles* $\boldsymbol{\eta} = (\eta_i)_{i=1}^n, \mathbf{z} = (z_i)_{i=1}^n \in \mathbb{R}^n$ to model the perceived importance of different nodes or regions of the network for the attacker and the defender, respectively. For example one may consider the case of uniform value profiles $\boldsymbol{\eta} = \mathbf{z} = \mathbf{1}$, up to the extreme scenario where the profiles are maximally concentrated on single highly strategic nodes, i.e. $\boldsymbol{\eta} = \mathbf{e}_i, \mathbf{z} = \mathbf{e}_k$ for some $i, k = 1, \dots, n$. As before, $\boldsymbol{\eta}$ and \mathbf{z} can be interpreted as Lagrange multipliers in a constrained optimization problem in which the two players operate targeting a given heterogeneous risk profile.

2.3 Stackelberg Equilibrium

An extensive game with perfect information is a model for sequential decision-making in which players act in a prescribed order and have complete knowledge of all previous actions taken by others. In particular, we consider a Stackelberg extensive game, where the defender moves first (*leader*) and the attacker makes their decision accordingly (*follower*).

In this setup, while the defender's strategy is defined by the choice of an action $\mathbf{q} \in S_d \subseteq [0, 1]^n$, the attacker's strategy is determined by a response function

$$\phi : S_d \ni \mathbf{q} \rightarrow \phi(\mathbf{q}) \in S_a, \quad (4)$$

that assigns an action to any possible choice of the defender, where we denoted as $S_a \subseteq [0, 1]^n$ the set of cyber-attack probability distributions over n nodes. We denote the set of possible response functions as R_a .

The proposed ordering is natural in our interpretation of the defender's action as a cyber-security investment — placing defenses and enhancing system resilience in anticipation of potential future attacks. Conversely, the opposite ordering would be more appropriate to model scenarios in which the defender, reacting to an attack that has already occurred, actively executes a defensive strategy to block it or mitigate its impact on the system. Although not addressed in the present paper, there are several situations in which it is worthwhile to consider a Stackelberg formulation where the attacker moves first. For example in the case of a *ransomware attack* through the network, the defender reacts by isolating compromised nodes or restoring data from backup [55]. In computer networks, after a *data exfiltration attack*, the defender reacts blocking nodes or filtering the suspicious traffic acting on links [43]. In the context of dynamic resource allocation, after a *distributed denial-of-service* moved saturating the network resources, the defender reacts reallocating resources [37]. Even *cyber kill chain* can be an example of Stackelberg attacker-first framework: the attacker starts with the first move sending malicious messages through network channels then the defender responds with countermeasures over the network such as blocking suspicious domains [32].

In a Stackelberg extensive game, a natural definition for an optimal pair of strategies $(\mathbf{q}^*, \phi^*(\cdot))$ is given by the following

Definition 2 (Strong Stackelberg equilibrium SSE). *In a Stackelberg game with utility functions \mathcal{U}_d and \mathcal{L}_d , a pair of strategies $(\mathbf{q}^*, \phi^*(\cdot))$, where $\mathbf{q}^* \in S_d$ is the defender's strategy and $R_a \ni \phi^* : S_d \rightarrow S_a$ is the attacker's response function, is a strong Stackelberg equilibrium (SSE) if:*

1. *The attacker plays a best response in each subgame:*

$$\mathcal{U}_a(\phi^*(\mathbf{q}); \mathbf{q}) \geq \mathcal{U}_a(\phi(\mathbf{q}); \mathbf{q}), \quad \forall \mathbf{q} \in S_d, \forall \phi \in R_a;$$

2. *The defender plays a best response:*

$$\mathcal{L}_d(\mathbf{q}^*; \phi^*(\mathbf{q}^*)) \leq \mathcal{L}_d(\mathbf{q}; \phi^*(\mathbf{q})), \quad \forall \mathbf{q} \in S_d;$$

3. *The attacker breaks ties optimality for the defender:*

$$\mathcal{L}_d(\mathbf{q}, \phi^*(\mathbf{q})) \leq \mathcal{L}_d(\mathbf{q}, \mathbf{f}^*), \quad \forall \mathbf{q} \in S_d, \mathbf{f}^* \in S_a^q,$$

where we denoted S_a^q as the set of the attacker best responses to \mathbf{q} , i.e. $S_a^q = \{\mathbf{f}^* \in S_a : \mathbf{f}^* = \arg \max_{\phi \in S_a} \mathcal{U}_a(\phi; \mathbf{q})\}$.

By definition, a Strong Stackelberg Equilibrium (SSE) is always a subgame perfect equilibrium [18] due to conditions 1 and 2. In the presence of multiple equilibria, given by the existence of multiple best response functions, condition 3 serves to select a subset of them. In general the Nash equilibrium of a two players strategic game differs from the SSE of the corresponding Stackelberg version of the game, meaning that the moves' order is crucial [29].

3 Results

3.1 Asymptotic Equilibrium and Emerging Network metrics

Let us define the risk measure of a node \mathcal{R}_i as the probability that the node i becomes infected, i.e.

$$\mathcal{R}_i(\mathbf{q}, \phi; \mathbf{A}) := \mathbb{P}_i(\mathbf{q}, \phi; \mathbf{A}), \quad (5)$$

where

$$\begin{aligned} \mathbb{P}_i(\mathbf{q}, \phi; \mathbf{A}) &:= \mathbb{E}_{\mathbf{X}, s} [\mathbb{I}(i \sim s \in \mathcal{T}(\mathbf{X}))] \\ &= \sum_{s=1}^n \phi_s \mathbb{E}_{\mathbf{X}} [\mathbb{I}(i \sim s \in \mathcal{T}(\mathbf{X}))], \end{aligned} \quad (6)$$

and $\mathbb{I}(\cdot)$ denotes the indicator function of a set. The expression $i \sim s \in \mathcal{T}(\mathbf{X})$ represents the event that node i is connected to the seed node s within the transmission subnetwork of susceptible nodes $\mathcal{T}(\mathbf{X})$, as in Definition 1.

In this context, the optimal security investment \mathbf{q}^* corresponding to a Strong Stackelberg Equilibrium (SSE) of the security game can be characterized using simple network metrics, which describe each node's vulnerability based on its position within the network topology. Let us define the 1-point and 2-points network protection metrics as follows.

Definition 3 (1-point protection). *Let \mathcal{G} be a network of n nodes. The 1-point protection is defined as the tensor $\mathbf{p}^1 = \{a_{ik}^j\}_{i,j,k=1}^n \in \{0, 1\}^{n^3}$, where each entry a_{ik}^j is given by*

$$a_{ik}^j = \begin{cases} 1 & \text{if } i \sim k \text{ in } \mathcal{G} \text{ and } i \not\sim k \text{ in } \mathcal{G} \setminus \{j\}, \\ 0 & \text{otherwise,} \end{cases}$$

and $\mathcal{G} \setminus \{j\}$ denotes the sub-network obtained by removing node j from \mathcal{G} . We define $a_{ii}^j = 0$, $\forall i \neq j$, and $a_{ij}^j = 1$.

The 1-point protection encodes whether the removal of a single node j can disrupt the connectivity between a pair of nodes (i, k) , initially connected, potentially blocking the spread of an infection between them. For example, in the network shown in Fig. 2, the potential contagion between nodes 3 and 6 can be prevented by removing (or immunizing) either node 5, so that $a_{36}^5 = 1$, or node 1, resulting in $a_{36}^1 = 1$. From the 1-point protection tensor, given two vectors $\mathbf{v}, \mathbf{w} \in \mathbb{R}^n$, we define its weighted reductions as

$$a_i^j(\mathbf{v}) := \sum_{k=1}^n a_{ik}^j v_k = \sum_{k=1}^n a_{ki}^j v_k \quad (7)$$

$$a^i(\mathbf{v}, \mathbf{w}) := \sum_{j,k=1}^n a_{jk}^i v_j w_k = \sum_{k=1}^n a_k^i(\mathbf{v}) w_k = \sum_j a_j^i(\mathbf{w}) v_j, \quad (8)$$

where we used that $a_{ik}^j = a_{ki}^j$ that also implies $a^i(\mathbf{v}, \mathbf{w}) = a^i(\mathbf{w}, \mathbf{v})$.

Definition 4 (2-points protection). Let \mathcal{G} be a network of n nodes. The 2-point protection is defined as the tensor $\mathbf{p}^2 = \{b_{ks}^{(i,j)}\}_{i,j,k,t=1}^n \in \{0,1\}^{n^4}$, where each entry $b_{ks}^{(i,j)}$ is given by

$$b_{ks}^{(i,j)} = \begin{cases} 1 & \text{if } k \sim s \text{ in } \mathcal{G}, \ a_{ks}^i = a_{ks}^j = 0, \ k \not\sim s \text{ in } \mathcal{G} \setminus \{i,j\}, \\ 0 & \text{otherwise,} \end{cases}$$

where a_{ks}^j denotes the entries of the 1-point protection tensor \mathbf{p}^1 of \mathcal{G} , and $\mathcal{G} \setminus \{i,j\}$ is the sub-network obtained by removing both nodes i and j from \mathcal{G} .

Unlike the 1-point protection, the 2-point protection captures whether the simultaneous removal of a pair of nodes (i,j) can disrupt the connectivity between another pair of nodes (k,s) , initially connected, in cases where the removal of either i or j alone is insufficient to cause such disruption. For example, in the network shown in Fig. 2, the removal (or immunization) of either node 2 or node 4 alone is not sufficient to prevent the potential contagion between nodes 3 and 6—that is, $a_{36}^2 = a_{36}^4 = 0$. However, the simultaneous removal of both nodes $(2,4)$ successfully blocks the connection, and thus $b_{36}^{(2,4)} = 1$. For a given pair of vectors $\mathbf{v}, \mathbf{w} \in \mathbb{R}^n$, we define

$$b_{ij}(\mathbf{v}, \mathbf{w}) := (1 - \delta_{ij}) \sum_{k,s} \left(b_{ks}^{(i,j)} - a_{ks}^i a_{ks}^j \right) v_k w_s. \quad (9)$$

The 1- and 2-point protection metrics identify the most strategic and cost-effective locations in the network where a potential infection can be locally blocked. Since they rely on the removal (or immunization) of only one or two nodes, these metrics suggest defense strategies that are both targeted and resource-efficient. As such, they provide actionable guidance on where to concentrate cyber defense efforts and allocate investments.

However, many other approaches exist to assess node importance in terms of system vulnerability and contagion prevention. For instance the previous framework could be generalized to define k -point protection for arbitrary values of k , allowing for the study of more complex cooperative defense strategies involving multiple nodes. Moreover, centrality-based measures—such as degree, betweenness, closeness, and k-core—have long been used to identify influential nodes [50], and recent work has proposed multi-attribute decision-making methods that integrate several structural indicators to provide a more comprehensive assessment [56]. What makes the 1- and 2-point protection metrics particularly relevant is that they emerge naturally from the analysis of Stackelberg equilibria in the security game introduced in this work. In fact, it holds the following

Theorem 1 (Asymptotic SSE). Consider a security Stackelberg game with contagion on a network \mathcal{G} of n nodes, defined by the attacker utility \mathcal{U}_a (2), the defender loss \mathcal{L}_d (3), a risk profile \mathcal{R} as in (5), and quadratic cost functions. If θ is sufficiently large, a SSE security investment satisfies

$$\mathbf{q}^* \sim^\alpha (\alpha \mathbb{I} - \mathbf{M})^{-1} \mathbf{s}, \quad (10)$$

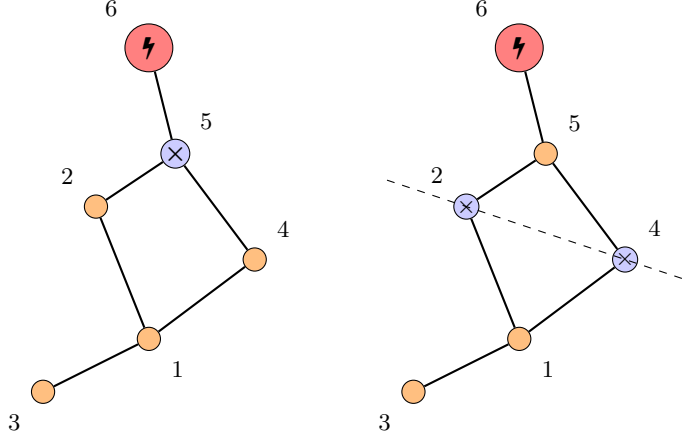


Fig. 2. Illustration of 1- and 2-point protection in a network. The potential contagion between nodes 3 and 6 can be prevented by removing (or immunizing) either node 5 (left panel), so that $a_{36}^5 = 1$, or node 1, resulting in $a_{36}^1 = 1$. In contrast, the removal of either node 2 or node 4 alone is not sufficient to block the contagion—i.e., $a_{36}^2 = a_{36}^4 = 0$ —but their simultaneous removal (right panel) successfully disrupts the connection, yielding $b_{36}^{(2,4)} = 1$.

where $\mathbf{M} = \mathbf{M}(\mathbf{z}, \boldsymbol{\eta}; \mathbf{p}^1, \mathbf{p}^2) \in \mathbb{R}^{n \times n}$ and $\mathbf{s} = \mathbf{s}(\mathbf{z}, \boldsymbol{\eta}; \mathbf{p}^1, \mathbf{p}^2) \in \mathbb{R}^n$ are defined by

$$\begin{aligned} s^i(\mathbf{z}, \boldsymbol{\eta}; \mathbf{p}^1, \mathbf{p}^2) &:= a^i(\mathbf{1}/n, \mathbf{z}), \\ M_{ij}(\mathbf{z}, \boldsymbol{\eta}; \mathbf{p}^1, \mathbf{p}^2) &:= b_{ij}(\mathbf{1}/n, \mathbf{z}) \\ &\quad - \frac{1}{\theta} \sum_{k=1}^n \left(a_k^i(\boldsymbol{\eta}) a_k^j(\mathbf{z}) - a^i(\mathbf{1}/n, \boldsymbol{\eta}) a^j(\mathbf{1}/n, \mathbf{z}) \right) \\ &\quad - \frac{1}{\theta} \sum_{k=1}^n \left(a_k^i(\mathbf{z}) a_k^j(\boldsymbol{\eta}) - a^i(\mathbf{1}/n, \mathbf{z}) a^j(\mathbf{1}/n, \boldsymbol{\eta}) \right) \end{aligned} \quad (11)$$

The notation $\mathbf{a} \sim^\alpha \mathbf{b}$ indicates that $\|\mathbf{a} - \mathbf{b}\| = o(1/\alpha^2)$ as $\alpha \rightarrow \infty$.

The proof of Theorem 1 is provided in Appendix 5 and builds upon a generalization of the results presented in [1]. Theorem 1 offers an explicit approximation of the defender's optimal cyber investment strategy, which becomes asymptotically exact in the limit $\alpha \rightarrow \infty$. This corresponds to a scenario in which the cost function dominates the optimization, and can therefore be interpreted as a low-budget regime for the defender. In fact, Eq. (10) can be expanded as

$$\mathbf{q}^* = \frac{1}{\alpha} \mathbf{s} + \frac{1}{\alpha^2} \mathbf{M} \mathbf{s} + o\left(\frac{1}{\alpha^2}\right), \quad (12)$$

indicating a vanishing optimal investment as $\alpha \rightarrow \infty$.

A key feature of this approximation is its dependence on the network topology solely through the network-based metric tensors \mathbf{p}^1 and \mathbf{p}^2 , which naturally emerge from the structure of the game and are combined properly according to the value profiles \mathbf{z} and $\boldsymbol{\eta}$.

Theorem 1 extends the results of [1], which are recovered as special cases. For instance, in the limit as $\theta \rightarrow \infty$, the utility function reduces to the cost $\mathcal{C}_a(\phi)$, compelling the attacker to adopt a uniform strategy $\phi^* = \mathbf{1}/n = (1/n, \dots, 1/n)$. In this regime, the problem simplifies to the social optimum under random, non-strategic attacks, as studied in [1] for $\mathbf{z} = \mathbf{1}$. Another special case arises by setting $\mathbf{z} = \mathbf{e}_i$ and $\boldsymbol{\eta} = \mathbf{1}/n$. Under these conditions, we obtain $a_k^i(\mathbf{z}) = a^i(\mathbf{1}/n, \mathbf{z}) = 1$, and $b_{ij}(\mathbf{1}/n, \mathbf{z}) = -(1 - \delta_{ij})a_i^j(\mathbf{1}/n)$. Consequently, the matrix M becomes

$$M_{ij} = -(1 - \delta_{ij})a_i^j(\mathbf{1}/n) - \frac{1}{\theta} \sum_k a_k^i(\mathbf{1}/n)(a_{ik}^j - a_i^j(\mathbf{1}/n)),$$

which characterizes the Nash equilibrium under uniform strategic attack, as analyzed in [1], where each node in the network acts as an individual player minimizing its own infection probability. Again in the limit as $\theta \rightarrow \infty$ we recover the Nash equilibrium under random uniform attack.

3.2 Paths of contagion and scalable solutions

The analytical expression provided by Theorem 1 offers a good approximation of the optimal investment in the small-budget regime. Nevertheless, it can serve as a benchmark strategy across a broader range of scenarios. Its main advantage lies in its computational simplicity, as it avoids solving the full optimization problem, which typically requires a costly numerical search for the true SSE.

The core challenge lies in computing the risk profile \mathcal{R} as in (5), which in turn determines the utility and loss functions to be optimized. Introducing the random variable

$$N_i^L(s, \mathbf{X}; \mathbf{A}) = \text{Card} \left(\{(i_1 = i, i_2, \dots, i_\ell = s) \mid A_{i_k i_{k+1}} = 1, X_{i_k} = 1, i_k \in \mathbb{N}_n, k \in \mathbb{N}_{\ell-1}, \ell \leq L\} \right) \quad (13)$$

as the number of different paths of maximum length L connecting a node i to the seed s in the transmission subnetwork $\mathcal{T}(\mathbf{X})$ of susceptible nodes, the infection probability can be written as

$$\begin{aligned} \mathbb{P}_i(\mathbf{q}, \phi; \mathbf{A}) &= \mathbb{E}_{\mathbf{X}, s} [\mathbb{I}(i \sim s \in \mathcal{T}(\mathbf{X}))] \\ &= \mathbb{E}_{\mathbf{X}, s} \left[\lim_{L \rightarrow \infty} \Theta(N_i^L(s, \mathbf{X}; \mathbf{A}) - 1) \right], \\ &= \lim_{L \rightarrow \infty} \mathbb{E}_{\mathbf{X}, s} [\Theta(N_i^L(s, \mathbf{X}; \mathbf{A}) - 1)], \end{aligned} \quad (14)$$

where $\Theta(\cdot)$ denotes the Heaviside step function which returns one if the argument is greater than zero, i.e. $N_i^L \geq 1$, and zero otherwise. In the second line of Eq. 14 we exploit the fact that, for a given $i \in \mathbb{N}_n$, the sequence of random variables

$(\Theta(N_i^L - 1))_{L \geq 0}$ converges pointwise to $\mathbb{I}(i \sim s \in \mathcal{T}(\mathbf{X}))$. Intuitively, a node i is connected to the seed in $\mathcal{T}(\mathbf{X})$ if there exists at least a path, of arbitrary large length L , linking them. In the last line, the application of the dominated convergence theorem justifies the exchange of limit and expectation. Following the definition of $N_i^L(s, \mathbf{X}; \mathbf{A})$, let us observe that the parameter L is not only a technical cut-off but admits a natural interpretation as propagation time. In fact, a path of length L can be regarded as a sequence of L successive transmissions of the infection through the network to which we can associate a unit of time. In this sense, the path length directly corresponds to the time required for the contagion to travel from the seed to another node. Considering paths of length at most L is therefore equivalent to assuming that the infection can propagate only within a finite time interval. While, in the limit $L \rightarrow \infty$, the model recovers the regime in which the contagion has unlimited time to diffuse. In this sense, L can be understood as the infection propagation time, which equips the model with an explicit dynamical dimension.

The form of Eq. 14 suggests the introduction of an entire class of risk measure defined in terms of a pair (f, L) as

$$\mathcal{R}_i^{(f,L)}(\mathbf{q}, \phi; \mathbf{A}) = \mathbb{E}_{\mathbf{X},s} [f(N_i^L(s, \mathbf{X}; \mathbf{A}))], \quad (15)$$

where f is an arbitrary non-decreasing activation function. If f is bounded one can also consider the limit $\mathcal{R}_i^f = \lim_{L \rightarrow \infty} \mathcal{R}_i^{(f,L)}$.

In general, if the activation function f is non linear, the expected value cannot be computed explicitly and must instead be evaluated numerically. The computational cost of this operation grows exponentially with the network size n . Conversely, if we consider a linear activation function, then the risk is expressed as the expected number of paths from the node to the seed, i.e.

$$\begin{aligned} \mathcal{R}_i^L(\mathbf{q}, \phi; \mathbf{A}) &= \mathbb{E}_{\mathbf{X},s} [N_i^L(s, \mathbf{X}; \mathbf{A})] = \mathbb{E}_{\mathbf{X},s} \left[\sum_{\ell=1}^L (\mathbf{A} \circ \mathbf{X} \mathbf{X}^T)_{is}^\ell \right] \quad (16) \\ &= \mathbb{E}_{\mathbf{X},s} \left[\sum_{\ell=1}^L \sum_{i_2, \dots, i_{\ell-1}=1}^n A_{ii_2} A_{i_2 i_3} \cdots A_{i_{\ell-1} s} X_i X_{i_2} \cdots X_{i_{\ell-1}} X_s \right] \\ &= \sum_{\ell=1}^L \sum_{i_2, \dots, i_{\ell-1}, s=1}^n \phi_s A_{ii_2} A_{i_2 i_3} \cdots A_{i_{\ell-1} s} \prod_{k \in \{i, i_2, \dots, i_{\ell-1}, s\}^{(1)}} (1 - q_k), \end{aligned}$$

where we denoted with $I^{(1)}$ the set of distinct occurrences of a set I . This quantity can be computed as efficiently as a matrix multiplication. Empirically, we observe that the results exhibit very low sensitivity to the cut-off parameter L . Therefore one can simply solve the optimization problem with $\mathcal{R} = \mathcal{R}^L$ with very small L to obtain optimal strategies that scale efficiently to large systems.

4 Numerical results

4.1 Efficient frontier

For any given defender and attacker value profiles \mathbf{z} and $\boldsymbol{\eta}$, the optimal defender strategy at the Stackelberg equilibrium provides a quantitative measure of the vulnerability associated with a specific network topology. This insight can be leveraged to guide the selection of system architectures that offer greater robustness.

Inspired by the classical Markowitz portfolio selection theory [40], we assess the robustness of different network topologies by computing the efficient frontier of the problem. Specifically, we scatter plot the system's global risk at equilibrium,

$$\mathcal{R}^*(\alpha; \mathbf{A}) := \sum_{i=1}^n z_i \mathcal{R}_i(\mathbf{q}^*(\alpha; \mathbf{A}), \phi^*(\mathbf{q}^*(\alpha; \mathbf{A})); \mathbf{A}), \quad (17)$$

highlighting its dependence on the network topology \mathbf{A} , against the corresponding defender's cost at equilibrium,

$$\mathcal{C}_d^*(\alpha; \mathbf{A}) := \mathcal{C}_d(\mathbf{q}^*(\alpha; \mathbf{A})), \quad (18)$$

for varying values of the Lagrange multiplier α . The resulting risk–cost plot illustrates the trade-off between investment and security: it shows the minimum cost the defender must incur to achieve a given level of system risk, or equivalently, the minimum achievable risk for a given admissible cost (i.e., the defender's budget). The security performance of different network topologies can thus be evaluated by comparing their respective efficient frontiers. The efficient frontier also serves as a powerful tool to compare the impact of different value profiles—that is, different attacker targeting regions and defender protection priorities—on a fixed system topology. By varying the allocation of value across nodes, we can assess how the equilibrium risk–cost trade-off shifts, providing insight into which regions of the network are most critical to secure under different threat scenarios.

Fig. 3 illustrates the efficient frontiers for a tree-structured network consisting of 121 nodes organized across four levels, with a branching ratio of 3. The risk measure used is the infection probability (5) and costs are quadratic. We consider different value profiles \mathbf{z} and attack distribution $\boldsymbol{\phi}$, each targeting a distinct level of the tree—from the root, i.e. $\mathbf{z}, \boldsymbol{\phi} = (1, 0, \dots, 0)$, to intermediate levels such as $\mathbf{z}, \boldsymbol{\phi} = (0, 1/3, 1/3, 1/3, 0, \dots, 0)$, and finally to the leaves, i.e. $\mathbf{z}, \boldsymbol{\phi} = (0, \dots, 1/81, \dots, 1/81)$. One can observe that, it generally appears easier for the defender to protect levels that are closer to the root, as the efficiency frontiers tend to rise with the distance from the root in the defender's value profile. However, the systemic risk is strongly affected by the attack distribution. In particular, the system appears less vulnerable when the attack starts from inner levels than the one deemed most important by the defender. The reason is that a smaller subset of nodes must be immunized in order to prevent infection spread.

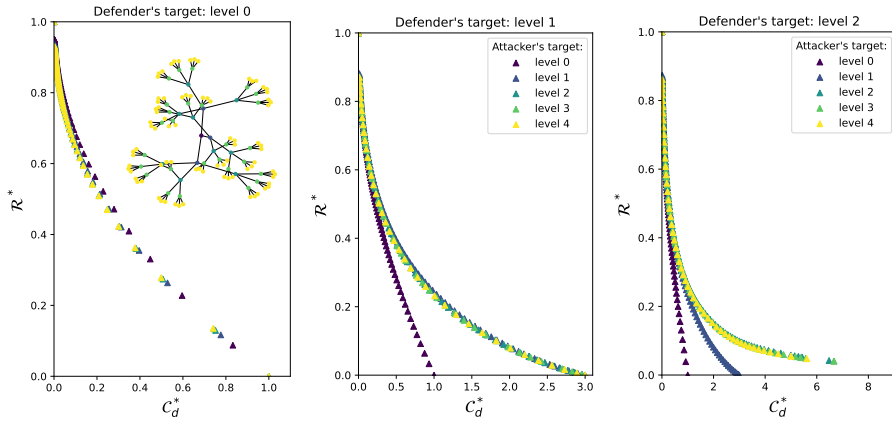


Fig. 3. Efficient frontiers for a tree network with 121 nodes, branching ratio 3, and 4 levels, are shown for different defender's value profile and attack distribution \mathbf{z} , ϕ concentrated on specific levels of the tree. Colors distinguish the different levels targeted by the attacker (see inset of the Left Panel). Each panel corresponds to a different defender's value profile, aiming to protect respectively the root (Left Panel), the first level (Central Panel), and the second level of the tree (Right Panel).

In contrast, when the attack originates from peripheral levels, the risk vanishes once the defender's budget is sufficient to immunize all nodes within the level of interest, regardless of the level targeted by the attacker.

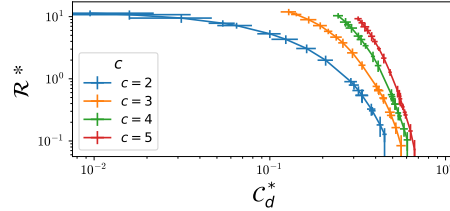


Fig. 4. Efficient frontiers for Erdos-Renyi random networks with different connectivity. The defender's cost is linear and the risk is $\mathcal{R} = \mathcal{R}^{L=4}$. The value profiles $\mathbf{z} = \boldsymbol{\eta} = \mathbf{1}$ are uniform.

Fig. 4 shows the efficient frontiers of random networks, generated as instances of the sparse Erdős–Rényi random graph model with connectivity c , representing the average number of neighbors per node. In this experiment, we assume a linear defender's cost and a risk $\mathcal{R} = \mathcal{R}^L$ as in Eq. (16) and the value profiles are uniform $\mathbf{z} = \boldsymbol{\eta} = \mathbf{1}$. We examine the effect of network topology by varying the connectivity level. Clearly, highly interconnected systems are both

more vulnerable and harder to defend, as infections can spread along multiple pathways and are difficult to contain.

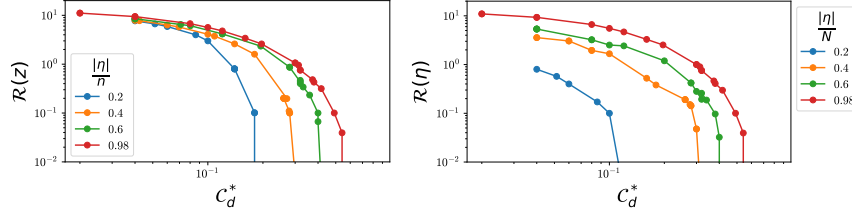


Fig. 5. Efficient frontiers for an Erdos-Renyi random network, with linear defender's cost and risk $\mathcal{R} = \mathcal{R}^{L=4}$. The defender's value profile $\mathbf{z} = \mathbf{1}$ is uniform while the attacker's value profile changes: $\boldsymbol{\eta} \in \{0, 1\}^n$, $|\boldsymbol{\eta}| := \sum_i \eta_i$. Left panel: optimal risk for the defender $\mathcal{R}^*(\mathbf{z}) = \sum_i z_i \mathcal{R}_i^*$. Right Panel: optimal risk for the attacker $\mathcal{R}^*(\boldsymbol{\eta}) = \sum_i \eta_i \mathcal{R}_i^*$

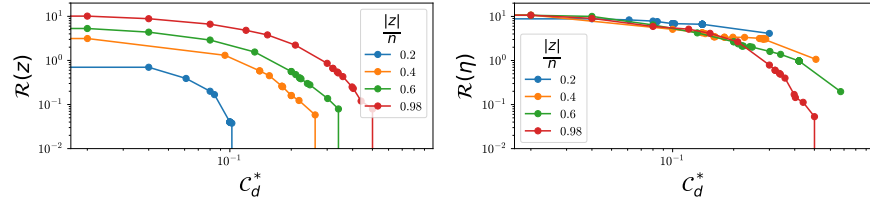


Fig. 6. Efficient frontiers for an Erdos-Renyi random network, with linear defender's cost and risk $\mathcal{R} = \mathcal{R}^{L=4}$. The attacker's value profile $\boldsymbol{\eta} = \mathbf{1}$ is uniform while the defender's value profile changes: $\mathbf{z} \in \{0, 1\}^n$, $|\mathbf{z}| := \sum_i z_i$. Left panel: optimal risk for the defender $\mathcal{R}^*(\mathbf{z}) = \sum_i z_i \mathcal{R}_i^*$. Right Panel: optimal risk for the attacker $\mathcal{R}^*(\boldsymbol{\eta}) = \sum_i \eta_i \mathcal{R}_i^*$

In Fig. 5, for a given Erdos-Renyi network and uniform defender value profile $\mathbf{z} = \mathbf{1}$, we investigate the effect of changing $\boldsymbol{\eta}$. In particular we choose $\boldsymbol{\eta} \in \{0, 1\}^n$, for different $|\boldsymbol{\eta}| := \sum_i \eta_i$, measuring the size of the subset of nodes that are valuable for the attacker. We measure both the defender's risk $\mathcal{R}^*(\mathbf{z}) = \sum_i z_i \mathcal{R}_i^*$ and the attacker's risk $\mathcal{R}^*(\boldsymbol{\eta}) = \sum_i \eta_i \mathcal{R}_i^*$, meaning the risk associated with the specific portion of the network relevant to the different players. The results indicate that a more localized attacker value profile leads to a lower systemic risk. Furthermore, the phase transition to zero risk occurs at a smaller defender's budget threshold.

Conversely, Fig. 6 shows the opposite situation in which the attacker value profile $\boldsymbol{\eta} = \mathbf{1}$ is uniform while the size of the subset of nodes that are valuable

for the defender changes, i.e. $\mathbf{z} \in \{0, 1\}^n$, for different $|\mathbf{z}| := \sum_i z_i$. Again it appears easier for the defender to protect portion of the network of smaller size, at a given budget. However the risk for the rest of the network increases, since the defensive strategy becomes suboptimal against systemic risk.

4.2 Cyber-deception strategy effects

A detailed examination of the optimal defender's strategy reveals how the investment is distributed across the various nodes of the network.

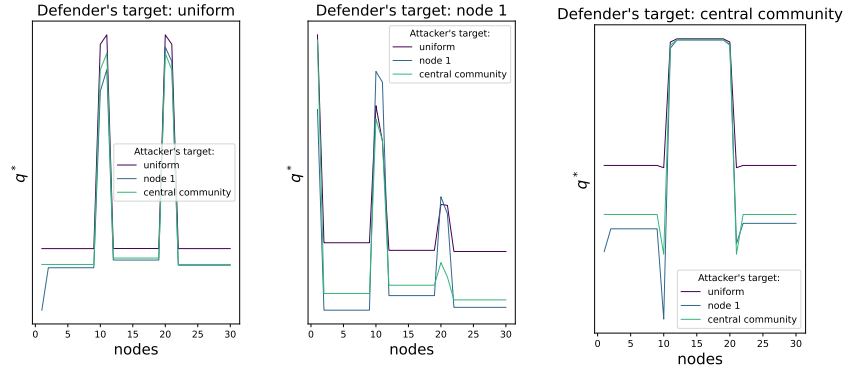


Fig. 7. Optimal investment pattern \mathbf{q}^* in a community network composed by three groups of 10 nodes, connected through the links (10, 11) and (20, 21), for different value profiles $\boldsymbol{\eta}$ and \mathbf{z} . Each panel corresponds to a different defender's value profile, aiming to protect respectively the whole system (Left Panel), the first node (Central Panel), and the central community (Right Panel). Different colors refers to different attacker's value profile.

In Fig. 7 for example we display the optimal investment pattern, computed used the approximation of Theorem 1 through protection metrics, in a network of 30 nodes with assortative communities, for different value profile scenarios. Specifically, we analyze three cases: (i) all nodes in the network have equal value, i.e. $\mathbf{z}, \boldsymbol{\eta} = (1/30, \dots, 1/30)$; (ii) node 1, which is a random node of the first community, is more valuable than the others, i.e. $\mathbf{z}, \boldsymbol{\eta} = (1, \dots, 0)$; (iii) the entire central community is targeted, i.e. $\mathbf{z}, \boldsymbol{\eta} = (0, \dots, 0, 1/10, \dots, 1/10, 0, \dots, 0)$. Across the three plots, the defender's value profile remains constant, whereas the attacker's profile changes.

Nodes that serve as inter-community bridges tend to be the most strategic to protect, given their key role in halting the spread of infections when immunized. As expected, when the value profiles correspond to cases (i) or (iii), the investment pattern appears symmetric with respect to the central community. In

contrast, this symmetry breaks when either z or η falls under case (ii). Furthermore, it is unsurprising that nodes in proximity to the defender’s most valuable assets attract greater security investment.

However, several unexpected effects become clearly observable. In particular, the attacker’s most valuable nodes consistently appear under-protected compared to others. Specifically, when node 1 becomes the most valuable for the attacker, its level of protection drops significantly (orange patterns); similarly, when the central community is the attacker’s primary target, its relative investment—compared to that of other communities—decreases (green pattern). These phenomena can be interpreted as instances of *cyber-deception* that favor the attacker, and are induced by the specific sequencing of actions in the Stackelberg framework. In fact, the attacker’s optimal strategy consists in avoiding a direct assault on the most valuable nodes. Instead, the attacker tends to select a seed that is relatively distant from them. This approach, combined with the sequential structure of the Stackelberg game, allows the attacker to mislead the defender, who ends up dispersing investments away from the actual targets. These effects arise because the defender does not have direct knowledge of the attacker’s specific value profile, having access only to the attacker’s optimal response function. Conversely, they are less pronounced when the attacker’s and defender’s value profiles—and thus their respective targets—coincide.

4.3 Contagion Dynamics

As previously discussed, optimal strategies have been derived within a game-theoretical framework that does not explicitly model contagion dynamics, but rather assumes that the epidemic has already reached its equilibrium, i.e. the infection has fully propagated through the transmission subnetwork of susceptible nodes.

However, our result can be evaluated under conditions of actual dynamic contagion, allowing us to assess its robustness against potential model misspecifications. To this end, we consider a benchmark class of epidemic models that describe the temporal evolution of infections across the network. Specifically, we consider a Markovian dynamics for the state evolution of nodes. The state at time t is defined by a vector $\sigma^t \in \{0, 1\}^n$, where σ_i^t is equal to one if the i -th node of the network is infected at time t , and zero otherwise.

We consider a setting in which, in the absence of security investments, each susceptible node ($(\sigma_i^t = 0)$) faces a probability of infection proportional to β at each time step, due to contact with each infected neighbors. At the same time, each infected node has a probability $1 - \gamma$ to recover thanks to its baseline security defenses. We therefore consider a general class of possible contagion dynamics defined by the transition rule

$$\sigma_i^{t+1} = \Theta \left[\sigma_i^t (\gamma - u) + (1 - \sigma_i^t) \left(\frac{\beta}{d_i} \sum_{j=1}^n A_{ij} \sigma_j^t - Z \right) \right], \quad (19)$$

where $d_i = \sum_j A_{ij}$ is the degree of the i -th node, i.e. the number of neighbors, and u, Z are random variables. In particular, $u \sim U(0, 1)$ and Z is a convex combination of an uniform random variable and a deterministic threshold $\delta \in [0, 1]$, i.e. $Z = \tau\delta + (1 - \tau)u$, $\tau \in [0, 1]$.

For $\tau = 1$, Eq. (19) represents a threshold contagion model [24, 54], in which a susceptible node becomes infected if the fraction of infected neighbors exceeds a given threshold δ . For $\tau = 0$, it reduces to a SIS model [44] in which the probability of contagion is

$$\mathbb{P}(\sigma_i^{t+1} = 1 | \sigma_i^t = 0, \sigma_{\setminus i}^t) = 1 - \prod_{j=1}^n (1 - \beta A_{ij} \sigma_j^t) = \beta \sum_{j=1}^n A_{ij} \sigma_j^t + o(\beta) \quad (20)$$

and the contagion rate β has been rescaled with the degree to ensure the r.h.s. term is in $[0, 1]$. Finally, setting the recovery rate $1 - \gamma$ to zero yields a classical SI model, where infected nodes remain infected indefinitely.

We assume that both players can influence the contagion dynamics. The defender mitigates the infection rate by investing in cyber-defense, which we model by rescaling the parameters as $\beta \rightarrow (1 - q_i)\beta$. The attacker, on the other hand, determines the initial distribution of threats. Accordingly, we define the initial state of the Markov process as

$$\mathbb{P}(\sigma^0) = \prod_{i=1}^n (\phi_i(1 - q_i))^{\sigma_i^0} (1 - \phi_i(1 - q_i))^{1 - \sigma_i^0}. \quad (21)$$

Here, $\phi_i(1 - q_i)$ represents the probability that node i is initially infected, modulated by the defender's investment level q_i .

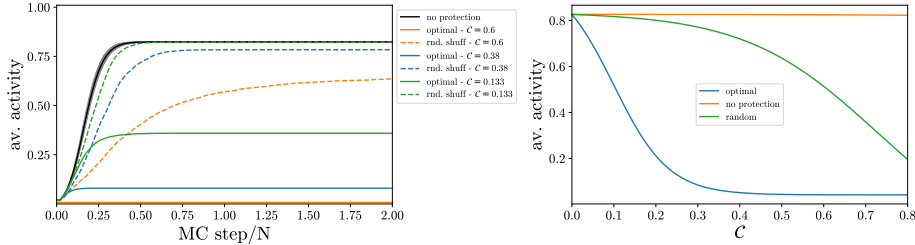


Fig. 8. SI contagion under different mitigation strategies: no protection, the proposed optimal strategy \mathbf{q}^* with uniform defender risk profile and a random reshuffling of the same budget. Left Panel: time evolution of the infection's size (average activity). Right Panel: asymptotic infection size as a function of the defender's budget.

In Fig. 8, we illustrate the effect of a mitigation strategy in random network where the infection evolves according to a SI dynamics. We compare the evolution of the fraction of infected nodes in the absence of security investments

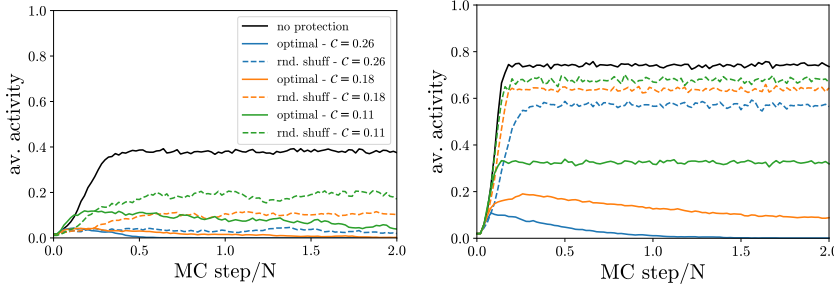


Fig. 9. Infection dynamics under different propagation rules, protection strategies and defender budgets. Left panel: SIS dynamics with $\gamma = 0.8$; Right Panel: threshold model with $\gamma = 0.9$ and $\delta = 0.2$. We compare three strategies: no protection (black), the proposed optimal strategy \mathbf{q}^* with uniform defender risk profile (full line) and a random reshuffling of the same budget (dashed line).

with that mitigated by the optimal allocation \mathbf{q}^* , derived from the security game equilibrium under uniform value profiles and a fixed budget. The results clearly show that the infection spreads more slowly and remains less extensive. The mitigating effect of this strategy outperforms that of a random reshuffling of the same investment budget, demonstrating its robustness even under contagion mechanism misspecification. The benefit of adopting an optimized strategy is particularly evident in the medium-budget regime, where investments have the potential to reduce infection but are insufficient to fully immunize the system. In this setting, an effective allocation becomes decisive. Fig. 9 shows that the previous results remain robust also under contagion dynamics governed by SIS and threshold models.

Conclusions

In this paper, we considered a general class of security games with contagion to study the optimal allocation of cybersecurity investments across the nodes of a networked system subjected to strategic attacks. Our analysis focused on the role of asymmetry between the risk profiles targeted by the attacker and the defender, as well as their heterogeneity.

We showed that, in a low-budget regime, the Stackelberg equilibria of the game can be approximated using simple network metrics that capture each node's ability to protect its neighbors and its value relative to the players' objectives. We also proposed a risk measure based on the number of contagion paths, making the optimization problem scalable for larger networks.

From numerical experiments, we showed that, unlike standard security games, the presence of contagion mechanisms fosters the emergence of optimal strategies involving cyber deception. We analyzed efficient frontiers to compare systemic risk across networks with different topologies and to highlight how asymmetry

and heterogeneity in risk profiles shape systemic resilience. Finally, we assessed the robustness of the proposed optimal strategies under alternative contagion dynamics.

Future perspectives will consider scenarios with incomplete or asymmetric information, examining how equilibrium strategies shift when defenders lack knowledge of the attacker's objectives and vice versa. Moreover, both attacker and defender are assumed to have perfect information about the system's architecture, which simplifies analysis but reduces realism. Assuming partial information on the network connections, especially for the attacker, would be a key perspective.

Another promising extension is a dynamic game formulation where the defender adapt their strategies as contagion unfolds. This could involve reallocating defenses across nodes or modifying the network topology, for example by disabling critical links. Coupling contagion dynamics with an iterative two-player game operating on different timescales would highlight a key missing element: the role of timing and the risks associated with delayed responses.

5 Appendix A: Proof of Theorem 1

Before proving Theorem 1, let us state some technical results. Throughout this appendix, let us denote $\mathbb{P}(\mathbf{q}, \phi; \mathbf{A})$ simply by $\mathbb{P}(\mathbf{q}, \phi)$. By the definition, we have the following decomposition of the probability that the node i becomes infected:

$$\mathbb{P}_i(\mathbf{q}, \phi) = (1 - q_i)\tilde{\mathbb{P}}_i(\mathbf{q}_{-i}, \phi), \quad (22)$$

where $(1 - q_i)$ is the probability that the node i is susceptible and the marginal $\tilde{\mathbb{P}}_i(\mathbf{q}_{-i}, \phi)$ is the probability that the infection reaches the node i then it does not depends on the pointwise security investment q_i , so \mathbf{q}_{-i} denotes the security profile \mathbf{q} without the entry q_i . Therefore, the probability that the node j , with $j \neq i$, becomes infected can be written as (Proposition 2, [1]):

$$\tilde{\mathbb{P}}_j(\mathbf{q}_{-j}, \phi) = \tilde{\mathbb{P}}_j(\mathbf{q}_{-\{i,j\}}, \phi) + (1 - q_i)Q_{ji}(\mathbf{q}_{-\{i,j\}}, \phi), \quad (23)$$

where $\tilde{\mathbb{P}}(\mathbf{q}_{-\{i,j\}}, \phi)$ is the probability that the infection reaches the node j through a path that does not contain the node i and $Q_{ji}(\mathbf{q}_{-\{i,j\}}, \phi)$ is the probability that the infection reaches the node j through a path that contains the node i conditioned i being susceptible. As a consequence, we obtain the following:

$$\frac{\partial}{\partial q_i} \mathbb{P}_j(\mathbf{q}, \phi) = -\delta_{ij}\tilde{\mathbb{P}}_i(\mathbf{q}, \phi) - (1 - \delta_{ij})(1 - q_j)Q_{ji}(\mathbf{q}, \phi), \quad (24)$$

where we have omitted the subscripts of \mathbf{q}_{-i} and $\mathbf{q}_{-\{i,j\}}$ for convenience of notation.

Lemma 1. *Given the security profile \mathbf{q} and the attack distribution ϕ , we have:*

$$\tilde{\mathbb{P}}_i(\mathbf{q}, \phi) = 1 - \sum_{j \neq i} \sum_t \phi_t a_{it}^j q_j + o(\|\mathbf{q}\|_\infty), \quad (25)$$

$$(1 - q_j)Q_{ji}(\mathbf{q}, \boldsymbol{\phi}) = \sum_t \phi_t \left(a_{jt}^i + \sum_{k \neq i} (b_{jt}^{(i,k)} - a_{jt}^i a_{jt}^k) q_k \right) + o(\|\mathbf{q}\|_\infty). \quad (26)$$

Proof. The claim is a direct generalization of Proposition 4 in [1].

Proof (Theorem 1).

Let us consider the optimization problem over the attacker's utility, with risk function defined in (5) and quadratic cost function $\mathcal{C}_a(\boldsymbol{\phi}) = \frac{1}{2} \sum_{i=1}^n \phi_i^2$, in order to obtain the best response to the defender's strategy \mathbf{q} :

$$\max_{\boldsymbol{\phi}} \mathcal{U}_a(\boldsymbol{\phi}; \mathbf{q}) = \max_{\boldsymbol{\phi}} \left(\sum_{i=1}^n \eta_i \mathbb{P}_i(\mathbf{q}, \boldsymbol{\phi}) - \frac{\theta}{2} \sum_{i=1}^n \phi_i^2 \right) \quad (27)$$

subjected to the constraints $\sum_i \phi_i = 1$ and $\phi_i \geq 0 \ \forall i = 1, \dots, n$. Let $L = L(\mathbf{q}, \boldsymbol{\phi}, \lambda, \mu)$ be the Lagrangian function, with parameters $\lambda \in \mathbb{R}$ and $\mu_i \in \mathbb{R}^+$ for all $i = 1, \dots, n$, related to the considered constrained optimization problem:

$$L(\mathbf{q}, \boldsymbol{\phi}, \lambda, \mu) = \sum_{i=1}^n \eta_i \mathbb{P}_i(\mathbf{q}, \boldsymbol{\phi}) - \frac{\theta}{2} \sum_{i=1}^n \phi_i^2 + \lambda \left(\sum_{i=1}^n \phi_i - 1 \right) + \sum_{i=1}^n \mu_i \phi_i.$$

Requiring the optimality condition:

$$\frac{\partial}{\partial \phi_i} L(\mathbf{q}, \boldsymbol{\phi}, \lambda, \mu) = \mathbb{P}_i(\mathbf{q}, \boldsymbol{\eta}) - \theta \phi_i + \lambda + \mu_i = 0, \quad \forall i = 1, \dots, n,$$

where

$$\mathbb{P}_i(\mathbf{q}, \boldsymbol{\eta}) = \sum_{s=1}^n \eta_s \mathbb{E}_{\mathbf{X}} [\mathbb{I}(i \sim s \in \mathcal{T}(\mathbf{X}))], \quad (28)$$

and imposing the constraints, we have that the best response $\boldsymbol{\phi}^*(\mathbf{q}) = (\phi_1^*(\mathbf{q}), \dots, \phi_n^*(\mathbf{q}))$ of the attacker is given by:

$$\phi_i^*(\mathbf{q}) = \frac{1}{n} + \frac{1}{\theta} \left(\mathbb{P}_i(\mathbf{q}, \boldsymbol{\eta}) - \frac{1}{n} \sum_{j=1}^n \mathbb{P}_j(\mathbf{q}, \boldsymbol{\eta}) \right), \quad i = 1, \dots, n. \quad (29)$$

Let us remark that the function in (28) directly relies the definition of the probability (6), however $\mathbb{P}_i(\mathbf{q}, \boldsymbol{\eta})$ is not a probability value since the weights η_1, \dots, η_n are not convex coefficients in general.

In order to estimate the optimal strategy \mathbf{q}^* of the defender, we are now interested in minimizing the defender's loss, with quadratic cost function $\mathcal{C}_d = \frac{1}{2} \sum_{i=1}^n q_i^2$, for $\boldsymbol{\phi} = \boldsymbol{\phi}^*$:

$$0 = \frac{\partial}{\partial q_i} \mathcal{L}_d(\mathbf{q}; \boldsymbol{\phi}^*) = \frac{\partial}{\partial q_i} \left(\sum_{s=1}^n z_s \mathcal{R}_s(\mathbf{q}, \boldsymbol{\phi}^*; \mathbf{A}) + \frac{\alpha}{2} \sum_{s=1}^n q_s^2 \right). \quad (30)$$

Let \mathbf{e}_s be the n -dimensional vector with 1 in the s -th entry and 0 elsewhere and $\mathbf{1}_n$ is the n -dimensional vector with $1/n$ in every entry. By definition (6), we have:

$$\mathbb{P}_i(\mathbf{q}, \mathbf{e}_k) = \mathbb{E}_{\mathbf{X}}[\mathbb{I}(i \sim k \in \mathcal{T}(\mathbf{X}))].$$

Therefore, the derivative of \mathcal{L}_d is

$$\begin{aligned} \frac{\partial \mathcal{L}_d}{\partial q_i} &= \alpha q_i + \sum_{k,s} z_s \phi_k^* \frac{\partial \mathbb{P}_s(\mathbf{q}, \mathbf{e}_k)}{\partial q_i} + \sum_{k,s} z_s \mathbb{P}_s(\mathbf{q}, \mathbf{e}_k) \frac{\partial \phi_k^*(\mathbf{q})}{\partial q_i} \\ &:= \alpha q_i + x_i + y_i. \end{aligned} \quad (31)$$

The term x_i is exactly the derivative computed for the social equilibrium in the random case, evaluated at ϕ^* , while the term y_i is due to the strategic nature of the problem and involves the derivative of $\phi^* = \phi^*(\mathbf{q})$. Let us compute the two terms applying (24):

$$\begin{aligned} x_i &= \sum_{k,s} z_s \phi_k^* \frac{\partial \mathbb{P}_s(\mathbf{q}, \mathbf{e}_k)}{\partial q_i} \\ &= -z_i \tilde{\mathbb{P}}_i(\mathbf{q}, \phi^*) - \sum_{s \neq i} z_s (1 - q_s) Q_{si}(\mathbf{q}, \phi^*) \\ &= -z_i \left(1 - \sum_{j \neq i} a_i^j(\phi^*) q_j \right) - \end{aligned} \quad (32)$$

$$\begin{aligned} &- \left(\sum_{j \neq i} z_j a_j^i(\phi^*) + \sum_{j \neq i} z_j \sum_s \sum_{k \neq i} \phi_s^* \left(b_{js}^{(i,k)} - a_{js}^i a_{js}^k \right) q_k \right) + o(\|\mathbf{q}\|_\infty) \\ &= - \sum_j z_j a_j^i(\phi^*) - \sum_{j \neq i} \sum_{sk} \phi_s^* z_k \left(b_{ks}^{(ij)} - a_{ks}^i a_{ks}^j \right) q_j + o(\|\mathbf{q}\|_\infty) \\ &= -a^i(\phi^*, \mathbf{z}) - \sum_{j \neq i} b_{ij}(\phi^*, \mathbf{z}) q_j + o(\|\mathbf{q}\|_\infty) \end{aligned} \quad (33)$$

where we used the approximations for $\tilde{\mathbb{P}}$ and Q provided by Lemma 1, $a_i^j = a_i^j(\phi)$, $a^i = a^i(\phi, \mathbf{z})$, and $b_{ij} = b_{ij}(\phi, \mathbf{z})$ are defined in (7), (8), and (9) respectively. By inserting $\phi^*(q)$, given in (29), and observing that

$$\phi_k^*(\mathbf{q}) = 1/n + \nabla \phi_k^*(0) \cdot \mathbf{q} + o(\mathbf{q}),$$

we have:

$$x_i = -a^i(1/n, \mathbf{z}) - \sum_{j \neq i} b_{ij}(1/n, \mathbf{z}) q_j - \sum_{jk} a_{jk}^i z_j \sum_s \frac{\partial \phi_k^*}{\partial q_s} \Big|_{\mathbf{q}=0} q_s + o(\|\mathbf{q}\|_\infty), \quad (34)$$

where the first two terms are exactly the ones appearing in the random case. The term y_i is

$$\begin{aligned}
y_i &= \sum_{k,s} z_s \mathbb{P}_s(\mathbf{q}, \mathbf{e}_k) \frac{\partial \phi_k^*(\mathbf{q})}{\partial q_i} = \sum_{k,s} z_s (1 - q_s) \tilde{\mathbb{P}}_s(\mathbf{q}, \mathbf{e}_k) \frac{\partial \phi_k^*(\mathbf{q})}{\partial q_i} \\
&= \sum_{ks} z_s (1 - q_s) \left(1 - \sum_{j \neq s} a_{sk}^j q_j \right) \frac{\partial \phi_k^*(\mathbf{q})}{\partial q_i} + o(\|\mathbf{q}\|_\infty) \\
&= \sum_{ks} z_s (1 - q_s) \frac{\partial \phi_k^*(\mathbf{q})}{\partial q_i} - \sum_{ks} z_s \sum_{j \neq s} a_{sk}^j q_j \frac{\partial \phi_k^*(\mathbf{q})}{\partial q_i} + o(\|\mathbf{q}\|_\infty) \\
&= - \sum_{ks} z_s \sum_{j \neq s} a_{sk}^j q_j \frac{\partial \phi_k^*}{\partial q_i} \Big|_{\mathbf{q}=0} + o(\|\mathbf{q}\|_\infty), \tag{35}
\end{aligned}$$

where we used that $\sum_k \phi_k^* = 1$ and that only $\partial_{q_i} \phi_k^*(0)$ contributes to the leading order. To make explicit x_i and y_i , we just need to compute the term

$$\begin{aligned}
\frac{\partial \phi_k^*}{\partial q_i} \Big|_{\mathbf{q}=0} &= \frac{\partial}{\partial q_i} \left(\frac{1}{n} + \frac{1}{\theta} \left(\mathbb{P}_k(\mathbf{q}, \boldsymbol{\eta}) - \frac{1}{n} \sum_j \mathbb{P}_j(\mathbf{q}, \boldsymbol{\eta}) \right) \right) \Big|_{\mathbf{q}=0} \\
&= \frac{1}{\theta} \left(\frac{\partial \mathbb{P}_k(\mathbf{q}, \boldsymbol{\eta})}{\partial q_i} - \frac{1}{n} \sum_j \frac{\partial \mathbb{P}_j(\mathbf{q}, \boldsymbol{\eta})}{\partial q_i} \right) \Big|_{\mathbf{q}=0} \\
&= \frac{1}{\theta} \left(-\delta_{ik} \tilde{\mathbb{P}}_i(\mathbf{q}, \boldsymbol{\eta}) - (1 - \delta_{ik})(1 - q_k) Q_{ki}(\mathbf{q}, \boldsymbol{\eta}) \right. \\
&\quad \left. - \frac{1}{n} \sum_j \left(-\delta_{ij} \tilde{\mathbb{P}}_i(\mathbf{q}, \boldsymbol{\eta}) - (1 - \delta_{ij})(1 - q_j) Q_{ji}(\mathbf{q}, \boldsymbol{\eta}) \right) \right) \Big|_{\mathbf{q}=0} \\
&= \frac{1}{\theta} \left(-\delta_{ki} - (1 - \delta_{ki}) a_k^i(\boldsymbol{\eta}) + \frac{1}{n} \sum_j (\delta_{ji} + (1 - \delta_{ji}) a_j^i(\boldsymbol{\eta})) \right) \\
&= \frac{1}{\theta} (a^i(1/n, \boldsymbol{\eta}) - a_k^i(\boldsymbol{\eta})). \tag{36}
\end{aligned}$$

By inserting it into (35), we have:

$$\begin{aligned}
y_i &= \frac{1}{\theta} \sum_{ks} z_s \sum_{j \neq s} a_{sk}^j q_j (a_k^i(\boldsymbol{\eta}) - a^i(1/n, \boldsymbol{\eta})) + o(\|\mathbf{q}\|_\infty) \\
&= \frac{1}{\theta} \sum_{k,s,j} z_s a_{sk}^j q_j (a_k^i(\boldsymbol{\eta}) - a^i(1/n, \boldsymbol{\eta})) + o(\|\mathbf{q}\|_\infty) \\
&= \frac{1}{\theta} \sum_j q_j \sum_k a_k^j(\mathbf{z}) (a_k^i(\boldsymbol{\eta}) - a^i(1/n, \boldsymbol{\eta})) + o(\|\mathbf{q}\|_\infty) \\
&= \frac{1}{\theta} \sum_j \left(\sum_k a_k^i(\boldsymbol{\eta}) a_k^j(\mathbf{z}) - a^i(1/n, \boldsymbol{\eta}) a^j(1/n, \mathbf{z}) \right) q_j + o(\|\mathbf{q}\|_\infty),
\end{aligned}$$

where, in the second line we used that we have zero if $j = s$. Using the same type of computation in Eq. (34) we obtain

$$x_i = -a^i(1/n, \mathbf{z}) - \sum_{j \neq i} b_{ij}(1/n, \mathbf{z}) q_j \quad (37)$$

$$+ \frac{1}{\theta} \sum_j \left(\sum_k a_k^i(\mathbf{z}) a_k^j(\boldsymbol{\eta}) - a^i(1/n, \mathbf{z}) a^j(1/n, \boldsymbol{\eta}) \right) q_j + o(\|\mathbf{q}\|_\infty). \quad (38)$$

Putting all together into (31) we get:

$$\frac{\partial \mathcal{L}_d}{\partial q_i} = \alpha q_i - a^i(1/n, \mathbf{z}) \quad (39)$$

$$\begin{aligned}
&- \sum_{j \neq i} b_{ij}(1/n, \mathbf{z}) q_j + \frac{1}{\theta} \sum_j \left(\sum_k a_k^i(\boldsymbol{\eta}) a_k^j(\mathbf{z}) - a^i(1/n, \boldsymbol{\eta}) a^j(1/n, \mathbf{z}) \right) q_j \\
&+ \frac{1}{\theta} \sum_j \left(\sum_k a_k^i(\mathbf{z}) a_k^j(\boldsymbol{\eta}) - a^i(1/n, \mathbf{z}) a^j(1/n, \boldsymbol{\eta}) \right) q_j + o(\|\mathbf{q}\|_\infty) \quad (40)
\end{aligned}$$

$$= \alpha q_i - s^i(\mathbf{z}, \boldsymbol{\eta}; \mathbf{p}^1, \mathbf{p}^2) - \sum_j M_{ij}(\mathbf{z}, \boldsymbol{\eta}; \mathbf{p}^1, \mathbf{p}^2) q_j + o(\|\mathbf{q}\|_\infty),$$

where the vector \mathbf{s} and the matrix \mathbf{M} are defined in (11), as a consequence the equilibrium \mathbf{q}^* satisfies (10).

References

1. Acemoglu, D., Malekian, A., Ozdaglar, A.: Network security and contagion. *Journal of Economic Theory* **166**, 536–585 (2016)
2. Acemoglu, D., Ozdaglar, A., Tahbaz-Salehi, A.: Systemic risk and stability in financial networks. *American Economic Review* **105**(2), 564–608 (2015)
3. Akey, P., Lewellen, S., Liskovich, I., Schiller, C.: Hacking corporate reputations. Rotman School of Management Working Paper (3143740) (2023)

4. Amir, E., Levi, S., Livne, T.: Do firms underreport information on cyber-attacks? evidence from capital markets. *Review of Accounting Studies* **23**(3), 1177–1206 (2018)
5. Aspnes, J., Chang, K., Yampolskiy, A.: Inoculation strategies for victims of viruses and the sum-of-squares partition problem. *Journal of Computer and System Sciences* **72**(6), 1077–1093 (2006)
6. Bachrach, Y., Draief, M., Goyal, S.: Contagion and observability in security domains. In: 2013 51st Annual Allerton Conference on Communication, Control, and Computing (Allerton). IEEE (2013). <https://doi.org/10.1109/Allerton.2013.6736610>
7. Bai, R., Lin, H., Yang, X., Wu, X., Li, M., Jia, W.: Stackelberg security games with contagious attacks on a network: Reallocation to the rescue. *Journal of Artificial Intelligence Research* **77**, 487–515 (2023)
8. Basilico, N., Gatti, N., Amigoni, F., et al.: Leader-follower strategies for robotic patrolling in environments with arbitrary topologies. In: Proceedings of the International Joint Conference on Autonomous Agents and Multi Agent Systems (AAMAS). pp. 57–64 (2009)
9. Caccioli, F., Barucca, P., Kobayashi, T.: Network models of financial systemic risk: a review. *Journal of Computational Social Science* **1**(1), 81–114 (2018)
10. Calice, G., Sala, C., Tantari, D.: Contingent convertible bonds in financial networks. *Scientific Reports* **13**(1), 22337 (2023)
11. Chan, H., Ceyko, M., Ortiz, L.: Interdependent defense games with applications to internet security at the level of autonomous systems. *Games* **8**(1), 13 (2017)
12. Cobos, E.V., Cakir, S.: A review of the economic costs of cyber incidents. World Bank Group, Working Paper (2024)
13. Cohen, R., Havlin, S.: Complex networks: structure, robustness and function. Cambridge university press (2010)
14. Crosignani, M., Macchiavelli, M., Silva, A.F.: Pirates without borders: The propagation of cyberattacks through firms' supply chains. *Journal of Financial Economics* **147**(2), 432–448 (2023)
15. Eling, M., Wirsfs, J.: What are the actual costs of cyber risk events? *European Journal of Operational Research* **272**(3), 1109–1119 (2019)
16. Fang, F., Nguyen, T.H.: Green security games: Apply game theory to addressing green security challenges. *ACM SIGecom Exchanges* **15**(1), 78–83 (2016)
17. Fang, F., Stone, P., Tambe, M.: When security games go green: Designing defender strategies to prevent poaching and illegal fishing. In: IJCAI. vol. 15, pp. 2589–2595 (2015)
18. Ferguson, T.S.: A course in game theory. World Scientific (2020)
19. Gai, P., Kapadia, S.: Contagion in financial networks. *Proceedings of the Royal Society A: Mathematical, Physical and Engineering Sciences* **466**(2120), 2401–2423 (2010)
20. Gan, J., Elkind, E., Kraus, S., Wooldridge, M.: Defense coordination in security games: Equilibrium analysis and mechanism design. *Artificial Intelligence* **313**, 103791 (2022)
21. Goffman, W., Newill, V.: Generalization of epidemic theory. *Nature* **204**(4955), 225–228 (1964)
22. Goldstein, J., Chernobai, A., Benaroch, M.: An event study analysis of the economic impact of it operational risk and its subcategories. *Journal of the Association for Information Systems* **12**(9), 1 (2011)
23. Goyal, S., Vigier, A.: Attack, defence, and contagion in networks. *The Review of Economic Studies* **81**(4), 1518–1542 (2014)

24. Granovetter, M.: Threshold models of collective behavior. *American journal of sociology* **83**(6), 1420–1443 (1978)
25. Iyer, S.R., Simkins, B.J., Wang, H.: Cyberattacks and impact on bond valuation. *Finance Research Letters* **33**, 101215 (2020)
26. Jamilov, R., Rey, H., Tahoun, A.: The anatomy of cyber risk. Tech. rep., National Bureau of Economic Research (2021)
27. Jiang, A.X., Procaccia, A.D., Qian, Y., Shah, N., Tambe, M.: Defender (mis) coordination in security games (2013)
28. Khouzani, M., Liu, Z., Malacaria, P.: Scalable min-max multi-objective cybersecurity optimisation over probabilistic attack graphs. *European Journal of Operational Research* **278**(3), 894–903 (2019). <https://doi.org/10.1016/j.ejor.2019.05.041>
29. Korzhyk, D., Yin, Z., Kiekintveld, C., Conitzer, V., Tambe, M.: Stackelberg vs. nash in security games: An extended investigation of interchangeability, equivalence, and uniqueness. *Journal of Artificial Intelligence Research* **41**, 297–327 (2011)
30. Kotidis, A., Schreft, S.: Cyberattacks and financial stability: Evidence from a natural experiment (2022)
31. Kotidis, A., Schreft, S.: The propagation of cyberattacks through the financial system: Evidence from an actual event. Available at SSRN 5087787 (2024)
32. Kour, R., Karim, R., Dersin, P.: Modelling cybersecurity strategies with game theory and cyber kill chain. *International Journal of System Assurance Engineering and Management* pp. 1–12 (2025)
33. Kumar, V.S.A., Parameswaran, S., Srinivasan, A., Vullikanti, A.: Existence theorems and approximation algorithms for generalized network security games. In: *Proceedings of the 2010 IEEE 30th International Conference on Distributed Computing Systems (ICDCS)*. pp. 132–143. IEEE (2010). <https://doi.org/10.1109/ICDCS.2010.20>
34. Latora, V., Nicosia, V., Russo, G.: *Complex networks: principles, methods and applications*. Cambridge University Press (2017)
35. Li, M., Tran-Thanh, L., Wu, X.: Defending with shared resources on a network. In: *Proceedings of the AAAI Conference on Artificial Intelligence*. vol. 34, pp. 2046–2053. AAAI Press (2020)
36. Liang, X., Xiao, Y.: Game theory for network security. *IEEE Communications Surveys & Tutorials* **15**(1), 472–486 (2012)
37. Liu, B., Xu, H., Zhou, X.: Stackelberg dynamic game-based resource allocation in threat defense for internet of things. *Sensors* **18**(11) (2018). <https://doi.org/10.3390/s18114074>, <https://www.mdpi.com/1424-8220/18/11/4074>
38. Lou, J., Smith, A.M., Vorobeychik, Y.: Multidefender security games. *IEEE Intelligent Systems* **32**(1), 50–60 (2017)
39. Manshaei, M.H., Zhu, Q., Alpcan, T., Baçsar, T., Hubaux, J.P.: Game theory meets network security and privacy. *Acm Computing Surveys (Csur)* **45**(3), 1–39 (2013)
40. Markowitz, H.M.: Portfolio selection, the journal of finance. *7* (1). N **1**, 71–91 (1952)
41. Nekovee, M., Moreno, Y., Bianconi, G., Marsili, M.: Theory of rumour spreading in complex social networks. *Physica A: Statistical Mechanics and its Applications* **374**(1), 457–470 (2007)
42. Newman, M.: *Networks*. Oxford university press (2018)
43. Nguyen, T., Wellman, M.P., Singh, S.: A stackelberg game model for botnet data exfiltration. In: Rass, S., An, B., Kiekintveld, C., Fang, F., Schauer, S. (eds.) *Deci-*

sion and Game Theory for Security. pp. 151–170. Springer International Publishing, Cham (2017)

44. Pastor-Satorras, R., Castellano, C., Van Mieghem, P., Vespignani, A.: Epidemic processes in complex networks. *Reviews of modern physics* **87**(3), 925–979 (2015)
45. Piccotti, L.R., Wang, H.: Informed trading in the options market surrounding data breaches. *Global Finance Journal* **56**, 100774 (2023)
46. Pita, J., Jain, M., Marecki, J., Ordóñez, F., Portway, C., Tambe, M., Western, C., Paruchuri, P., Kraus, S.: Deployed armor protection: the application of a game theoretic model for security at the los angeles international airport. In: Proceedings of the 7th international joint conference on Autonomous agents and multiagent systems: industrial track. pp. 125–132 (2008)
47. Roy, S., Ellis, C., Shiva, S., Dasgupta, D., Shandilya, V., Wu, Q.: A survey of game theory as applied to network security. In: 2010 43rd Hawaii international conference on system sciences. pp. 1–10. IEEE (2010)
48. Shieh, E., An, B., Yang, R., Tambe, M., Baldwin, C., DiRenzo, J., Maule, B., Meyer, G.: Protect: A deployed game theoretic system to protect the ports of the united states. In: Proceedings of the 11th international conference on autonomous agents and multiagent systems-volume 1. pp. 13–20 (2012)
49. Sinha, A., Fang, F., An, B., Kiekintveld, C., Tambe, M.: Stackelberg security games: Looking beyond a decade of success. *IJCAI* (2018)
50. Song, J., Wang, G.: Identifying influential nodes in complex contagion mechanism. *Frontiers in Physics* **11**, 1046077 (2023)
51. Strogatz, S.H.: Exploring complex networks. *nature* **410**(6825), 268–276 (2001)
52. Tambe, M.: Security and game theory: algorithms, deployed systems, lessons learned. Cambridge university press (2011)
53. Tsai, J., Nguyen, T., Tambe, M.: Security games for controlling contagion. In: Proceedings of the AAAI Conference on Artificial Intelligence. vol. 26, pp. 1464–1470 (2012)
54. Watts, D.J.: A simple model of global cascades on random networks. *Proceedings of the National Academy of Sciences* **99**(9), 5766–5771 (2002)
55. Yin, T., Sarabi, A., Liu, M.: Deterrence, backup, or insurance: Game-theoretic modeling of ransomware. *Games* **14**(2) (2023). <https://doi.org/10.3390/g14020020>, <https://www.mdpi.com/2073-4336/14/2/20>
56. Zhang, Y., Lu, Y., Yang, G., Hang, Z.: Multi-attribute decision making method for node importance metric in complex network. *Applied Sciences* **12**(4), 1944 (2022)
57. Zhang, Y., Malacaria, P.: Keep spending: Beyond optimal cyber-security investment. In: 2023 IEEE 36th Computer Security Foundations Symposium (CSF). pp. 363–376. IEEE (2023). <https://doi.org/10.1109/csf57540.2023.00024>